17th World Conference on Earthquake Engineering, 17WCEE
Sendai, Japan - September 13th to 18th 2020

SCENARIO-BASED RESILIENCE ASSESSMENT OF COMMUNITIES WITH INTERDEPENDENT CIVIL INFRASTRUCTURE SYSTEMS

N. Blagojević[(1)], J. Kipfer[(2)], M. Didier[(3)], B. Stojadinović[(4)]

[(1)] *PhD Student, Institute of Structural Engineering, ETH Zurich, blagojevic@ibk.baug.ethz.ch*
[(2)] *MSc Student, ETH Zurich, jkipfer@student.ethz.ch*
[(3)] *Post-Doctoral Researcher, Institute of Structural Engineering, ETH Zurich, didier@ibk.baug.ethz.ch*
[(4)] *Professor, Institute of Structural Engineering, ETH Zurich, stojadinovic@ibk.baug.ethz.ch*

Abstract

Civil infrastructure systems (CISs) supply the communities with essential resources and services, such as electric power, potable water, telecommunication and transportation. Extreme events, such as earthquakes, can cause disruptions to these systems resulting in significant direct and indirect financial and societal losses. Increasing disaster resilience of CISs reduces the negative effects of such events on communities. However, in order to improve CIS and community disaster resilience, it first it needs to be quantified, so that various strategies for resilience improvement can be devised and evaluated.

This paper presents a model for quantifying the seismic resilience of communities with interdependent civil infrastructure systems. The model comprises four modules: the hazard module, the vulnerability module, the functional recovery module and the resilience quantification module. The hazard module is used to assess the intensity measures of a considered scenario earthquake at the geographic locations of CIS components. Ground motion prediction equations, and transient and permanent ground deformation models are used to estimate the peak ground acceleration, peak ground velocity and peak ground deformation, respectively. The vulnerability module links these measures to component damage states using seismic vulnerability curves. Due to the suffered damage, functionality of the components decreases. Additionally, certain components rely on the resources and services provided by other CISs. For example, a water pump needs electric power to operate. Such interdependencies between CISs are explicitly modeled using an iterative flow-based approach as they can cause further decreases of component functionality through feedback loops and cascading effects. The functional recovery module simulates the component repair process and restoration of component and system functionality using pre-assigned repair rates. Finally, the Re-CoDeS method is used to compute the unmet demand for a CISs service over time and thereby quantify the resilience (or lack thereof) of the considered CISs. In this paper, a virtual community served by three interdependent CISs is exposed to a scenario earthquake. The presented model is then used to quantify the seismic resilience of this system of systems and evaluate the effects of CIS interdependency.

Keywords: vulnerability functions, recovery, interdependency, resilience, civil infrastructure systems

1. Introduction

Extreme events, such as earthquakes, can damage civil infrastructure systems (CISs), preventing them from delivering essential resources and services to the communities they serve. The more damage CISs suffer and the longer they are out of service, the larger are the expected societal and financial losses of the communities they serve. Therefore, strategies that minimize both post-disaster direct damage and downtime of the CISs are needed. Several government agencies and institutions have suggested that increasing disaster resilience of the CISs is the most appropriate strategy [1–4]. Notably, models that simulate the (post-)disaster behavior of CISs and quantify their resilience are needed to develop and test strategies for increasing CIS disaster resilience [5]. However, simulating the (post-) disaster behavior of a CIS is a challenging task. A CIS is a complex, site-specific system, usually composed of many spatially distributed and interacting components. Furthermore, these components can be of different age, have various properties and even be managed by different entities.

When estimating the seismic resilience of a community, seismic intensity measures (e.g., peak ground acceleration, PGA) and the vulnerability of the CIS (component- and system-wise) to the considered seismic hazard must be estimated first. Since estimating resilience includes estimating the ability of a system to bounce back, to recover to its pre-disaster or to a new post-disaster state, modelling the process of component and system recovery from damage is essential. Recovery models are used to assess the evolution of damage and functionality of the considered system over the recovery period [6]. Finally, a method to quantify seismic resilience is needed. At this time, no broadly accepted methodology for quantifying the seismic resilience of a CIS exists. However, most of the existing methodologies are based on the framework proposed by the Multidisciplinary Center for Earthquake Engineering Research (MCEER), in that the disaster resilience of a system can be quantified by following its functionality (or lack thereof) over time after a disaster [7].

Communities rarely rely on the resources and services supplied by a single independent CIS. Modern communities are served by multiple interdependent CISs, whose functionality not only affects the daily life of the inhabitants of the community but also the functioning of other CISs. For example, a base transceiver station needs electric power supplied by the electric power supply system to operate. Neglecting CIS interdependency in evaluating community disaster resilience often results in optimistic estimates, since interdependencies increase the vulnerability of CISs [8]. Hence, a model used to quantify the seismic resilience of CISs must take into account the interdependency between the CISs.

2. Model Description

In the following, a model to estimate the resilience of a system exposed to a seismic hazard is presented. A system can be a CIS, a subsystem of a CIS, a part of the community or the entire community. In this study, the considered system is the entire community supplied with three interdependent CISs. Systems are composed of components. A component can be a facility belonging to a CIS (e.g. electric power plant) or a building stock unit. Links (e.g. pipes and power lines) and bridges are used to transfer the resources and services among components. The resources and services (e.g. electric power, potable water) produced and consumed in the system are labeled R/S, for convenience. The model consists of four modules: the hazard module, the vulnerability module, the functional recovery module and the resilience quantification module (Figure 1).

The hazard module estimates the intensity measures of a seismic event. Inputs to the hazard module are hazard-specific properties of the considered region (e.g., fault position, soil type, topology etc.) and the characteristics of the earthquake (e.g., moment magnitude, location of the epicenter etc.). Outputs are spatially distributed intensity measures, such as the PGA, the peak ground velocity (PGV) and the peak ground displacement (PGD). The outputs of the hazard module serve as the inputs to the vulnerability module. In the vulnerability module, the (probability of) a component being in a certain damage state is assessed based on the intensity measures obtained from the hazard module and seismic vulnerability curves associated with the system's components.

The damage states of the components, obtained from the vulnerability module, serve as input to the functional recovery module, which then simulates the functional recovery of the components during the recovery time. At each point in time, the output of this module is the functionality level of the components of the system. Finally, the resilience quantification module uses the functional recovery module outputs to quantify the resilience of the community. The exact functioning of the modules is explained next, using a virtual case study as an illustrative example.

Figure 1: Proposed model structure

© The 17th World Conference on Earthquake Engineering

3. Virtual Case Study

In the following, the hazard and the vulnerability module of the proposed model are described in detail using a virtual case study as an example. The functional recovery and the resilience quantification module are described in [9, 10] using the same case study. The setup of the proposed virtual community is given in Figure 2a [11]. It consists of the building stock (BS) and three interdependent CISs: Electric Power Supply System (EPSS), Cellular Communication System (CCS), and Water Supply System (WSS). The CISs are, in general, composed of suppliers (i.e., facilities that produce or make available a R/S), and links and bridges, which transfer the R/Ss to the users. The users can be BS units (representing the R/S demand of the inhabitants of the community) or other CIS facilities, which need specific R/Ss to operate (e.g., a water pump needs electric power to operate).

A detailed description of the virtual community and the modeling simplifications are provided in [9, 11]. The simplified EPSS consists of Electric Power Plants (EPPs) that produce electric power (measured in MWh) and power transmission lines that transfer the electric power to the users. The simplified CCS consists of Base Transceiver Stations (BTSs) that supply the users with wireless cellular communication (low level communication, LLC) and Base Station Controllers (BSCs) that control the wireless cellular traffic between the BTSs (high level communication, HLC). The cellular communication services are measured in Erlang [E] [12]. The simplified WSS consists of Potable Water Facilities (PWFs) and Cooling Water Facilities (CWFs). PWFs produce or make available potable water and transfer it to the users using water pipes. CWFs produce cooling water, which is transferred using cooling water pipes to the users. The potable water and cooling water quantities are measured in Mega Liters per day [Ml/day]. The BS consists of building stock units. Each building stock unit is assumed to provide housing for 400 inhabitants.

The virtual community is discretized into localities (Figure 2a). A locality can contain facilities or building stock units (e.g. Locality 303) or serve as an intersection between links (e.g. Locality 206). Localities are connected with links that transfer the R/Ss between localities. Transfer of R/Ss inside a locality is unconstrained. Bridges connecting localities 201 to 301 and 301 to 302 carry links (pipes and power lines) such that bridge damage can cause link damage and lead to interruptions in the transfer of electric power and potable and cooling water.

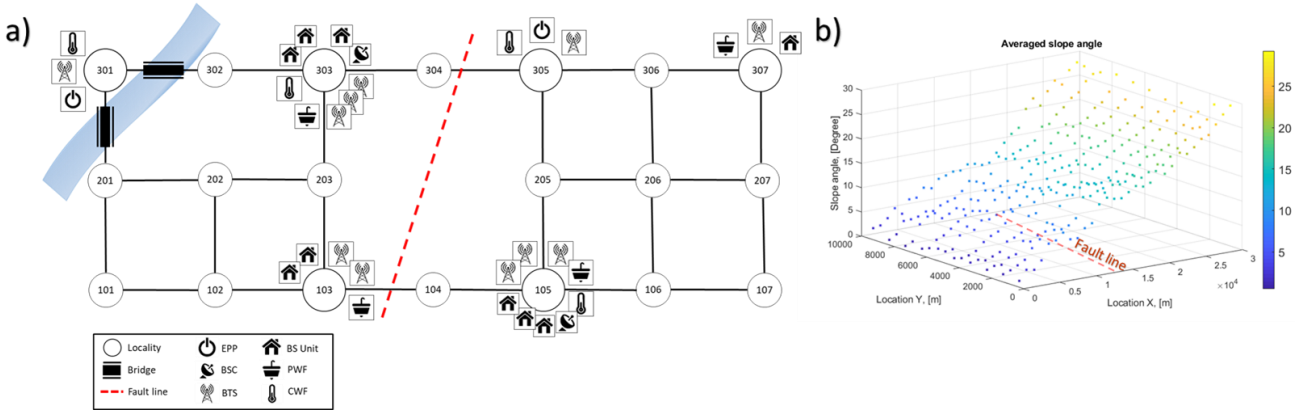

Figure 2: Virtual community set-up (a) and topography (b)

3.1.1 Hazard module

The community is exposed to a seismic hazard, generated by a linear strike-slip earthquake fault located in the middle of the community (Figure 2a). The seismic hazard model used here is an adaptation of the hazard model developed by Bellagamba [13]. The studied region (dimension 30km by 10km) is discretized into clusters for the purpose of hazard computation, each with a tributary area of 1km by 1km. For each cluster, the input parameters for the hazard model (e.g., topography, soil type, groundwater level, etc.) are defined as follows.

© The 17th World Conference on Earthquake Engineering

The topography of the region of interest is characterized by the average slope angle of each cluster (Figure 2b). Areas with higher slope angles are assumed to be mountains, while the areas with lower slope angles are assumed to be plains. Soil types are adopted according to the Eurocode 8 [14] soil type classification (Figure 3a). The geological age is assumed to be Holocene. The time-averaged shear-wave velocities are assigned to each cluster based on its soil type [13]. The soil of the clusters adjacent to the river is affected by the groundwater, as the presence of groundwater influences the probability of liquefaction [15]. It is assumed that depth of the groundwater is 3m, and that it can be found in clusters with soil types B, C and D which are not in the river.

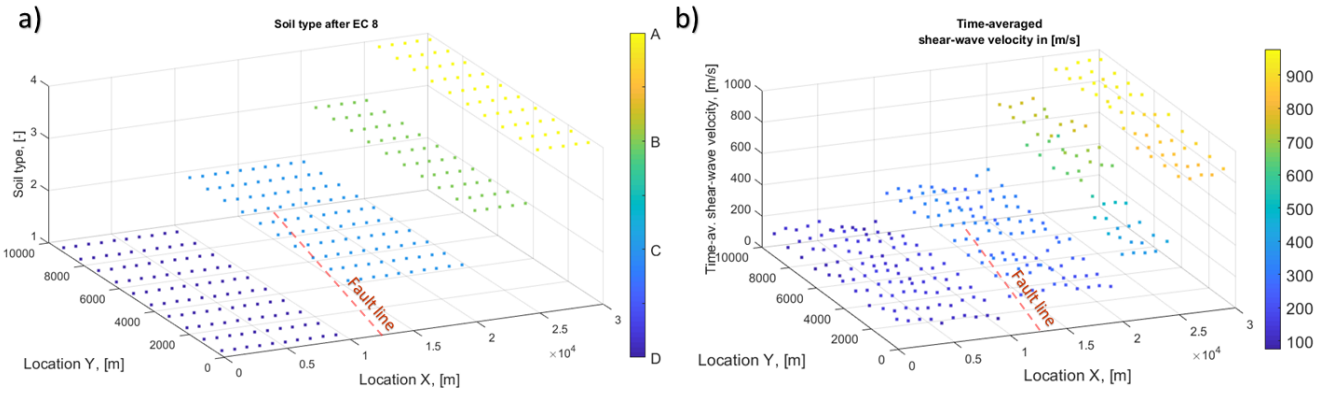

Figure 3: Soil types and shear-wave velocities of the virtual community

The earthquake fault, the source of the seismic hazard in the virtual community, is defined by its coordinates and type. The rupture length is a function of the earthquake moment magnitude and the fault type, and is calculated according to Kramer [16]. The Joyner-Boore distance [17] is used to define the distance from the rupture to the site of interest. The estimates of PGD account for liquefaction [15], ground settlement [15], lateral spreading [15], landslides [18] and faulting [19]. Ground motion prediction equations defined by Akkar et al. [20] are used to get the spatial distribution of the PGAs on the surface, including the soil amplification effects. Intra-event residual correlation is accounted for using the model by Esposito and Iervolino [21, 22]. The PGA is adopted as the first intensity measure, and the PGV is sampled from a conditional distribution dependent on the PGA, using the model of Iervolino et al. [23]. The output of the hazard module are the ground motion intensity measures (PGA, PGV and PGD) for each cluster of the studied region.

3.1.2 Vulnerability module

Seismic vulnerability curves are used to estimate the probability of damage of a component given the seismic hazard intensity measure at its location. The ground motion intensity measures from the cluster closest to the location of the considered component are used.

Table 1 summarizes the parameters of the lognormal seismic vulnerability curves used for the different components considered in this case study. It is assumed that all components are unanchored. The parameters of the vulnerability curves for the EPPs, BSCs, BS units and PWFs are taken from HAZUS [15], using the PGA as the hazard intensity measure. The damage state of a BTS depends on the damage state of the building on which it is located. Here, it is assumed that BTSs are located on top of 5-story RC shear wall buildings (HAZUS C2M building type) and that the damage state of the BTS corresponds to the damage state of the building. It is assumed that CWFs have the same vulnerability as PWFs. For bridges, vulnerability curves are obtained from the SYNER-G project database [24]. Each damage state is linked to a damage level (Table 1), representing the physical degree of damage of the component. While damage states are discrete, damage levels are continuous values from 0 (no damage) to 1 (complete damage). Damage levels are used to measure the level of physical damage of a component right after an earthquake as well as to track the recovery of the component over time.

© The 17th World Conference on Earthquake Engineering

Ground motion intensity measures PGVs and PGDs observed at the pipe location and pipe repair rate [15] are used to determine the number of expected breaks and leaks in the pipe segments. It is assumed that a leak reduces the functionality of a pipe segment by 20%, causing 20% of the water passing through the pipe to be lost. A break in a pipe segment leads to 0% functionality: the segment is fully damaged and cannot be used. Ductile pipes are assumed. Power transmission lines are assumed not to be damaged by the earthquake.

Table 1: Seismic vulnerability curve parameters

Component	Size	Characteristics	Damage state	Associated damage level	Median (g)	$\lambda(g)$	ζ
EPP [15]	Small (<200 MW)	Unanchored components (EPP2)	Minor	0.05	0.1	-2.30	0.55
			Moderate	0.25	0.21	-1.56	0.55
			Extensive	0.75	0.48	-0.73	0.50
			Complete	1.0	0.78	-0.25	0.50
BSC [15]	-	Unanchored components	Minor	0.1	0.13	-2.04	0.55
			Moderate	0.5	0.26	-1.35	0.5
			Extensive	1.0	0.46	-0.78	0.62
			Complete	1.0	1.03	0.03	0.62
BTS [15]	5 story RC shear wall building (C2M)	-	Slight	0.1	0.17	-1.77	0.64
			Moderate	0.5	0.36	-1.02	0.64
			Extensive	0.8	0.87	-0.14	0.64
			Complete	1.0	1.95	0.67	0.64
CWF and PWF [15]	Small (<38 Ml/d)	Small pumping plants with unanchored components (PPP2)	Minor	0.1	0.13	-2.04	0.6
			Moderate	0.5	0.28	-1.27	0.5
			Extensive	1.0	0.66	-0.42	0.65
			Complete	1.0	1.5	0.41	0.8
BS [15]	5 story RC shear wall building (C2M)	Moderate-code Seismic Design Level	Slight	0.25	0.17	-1.77	0.64
			Moderate	0.5	0.36	-1.02	0.64
			Extensive	0.75	0.87	-0.14	0.64
			Complete	1.0	1.95	0.67	0.64
Bridge [24]	Single Span Concrete Girder	-	Minor	0.05	0.35	-1.05	0.85
			Moderate	0.1	1.33	0.28	0.86
			Extensive	1.0	1.83	0.6	0.87
			Complete	1.0	2.5	0.92	0.9

© The 17th World Conference on Earthquake Engineering

3.1.3 Functional recovery module

Once the initial component damage states are estimated, the recovery times of the components are sampled from a normal distribution, whose parameters are given in Table 2. The parameters are taken from HAZUS [15]. Since no data regarding the BS units and BTS recovery time could be found in literature, the values are estimated by the authors (Table 2). It is assumed that a pipe leak and a pipe break take one and two days to fix, respectively.

The damage level of the component decreases at each time step of the system recovery simulation (the time step is set to one day in this case study) by the value of the repair rate. The repair rate is adopted so that the component recovers (i.e. reduces its damage level to zero) in the sampled recovery time.

Due to damage, the functionality of a component decreases affecting its supply capacity (i.e. how much R/S a component is producing) and its demand (i.e. how much R/Ss a component needs to operate). Functionality of a component is described using a functionality level, which depends on the damage level of a component, on the component type, and on the availability of the R/Ss the component needs to operate [9]. Functionality level can vary from 0, corresponding to no functionality, to 1, corresponding to full (initial) functionality. Supply capacity is proportional to the functionality level of components, while the relation between the functionality level and the demand depends on the component type and is explained in detail in [9].

In some cases, the description of the damage state does not offer any explanation regarding the functionality of the component. For example, the description of the extensive damage state of an EPP is "considerable damage to motor driven pumps, or considerable damage to large vertical pumps, or by the building being in extensive damage state" [15]. Therefore, assumptions have to be made linking damage states to damage levels and then to functionality levels, which in turn relate to changes in the supply capacities and demands of facilities and building stock units, as explained in [9, 11].

Apart from the damage level, functionality of a component depends on the availability of the R/Ss produced by other CISs that the component needs to operate – the physical interdependency [25]. To account for the decrease of functionality due to the CIS interdependency, an iterative flow-based approach is used. If at the current time step of the recovery simulation a component cannot be supplied by the R/Ss it needs to operate, it does not function. An iteration is used to examine possible sequences of component R/Ss demand and function in each time step to discover feedback loops that may lead to a number of components losing the ability to function in a cascading manner. The details regarding the method used to account for the interdependencies and the interdependency properties of the components can be found in [9, 11].

However, the damage states described in HAZUS implicitly consider interdependency between CISs. For example, the moderate damage state of a water pumping plant is defined as "the loss of electric power for about a week, considerable damage to mechanical and electrical equipment, or moderate damage to buildings" [15]. By including the "loss of electric power for a week" in the damage state description, the damage state definitions are implicitly including the interdependency effects between CISs together with the damage of the equipment. Hence, models that explicitly simulate interdependencies between CISs, like the model presented in this paper, have a risk of double-counting component inoperability due to interdependencies between CISs.

Table 2: Component recovery times

Component	Damage State	Mean [days]	Standard deviation [days]
EPP	Slight	0.5	0.1
	Moderate	3.6	3.6
	Extensive	22	21
	Complete	65	30

© The 17th World Conference on Earthquake Engineering

BSC	Slight	0.5	0.2
	Moderate	1	1
	Extensive	7	7
	Complete	40	40
BTS	Slight	2	2
	Moderate	5	5
	Extensive	20	20
	Complete	150	150
CWF and PWF	Slight	0.9	0.3
	Moderate	3.1	2.7
	Extensive	13.5	10
	Complete	35	18
BS	Slight	2	2
	Moderate	5	5
	Extensive	20	20
	Complete	150	150
Bridge	Slight	0.6	0.6
	Moderate	2.5	2.7
	Extensive	75	42
	Complete	230	110

3.1.4 Resilience quantification module

The Re-CoDeS framework is used to quantify the resilience of the community [26–28]. In Re-CoDeS, the Lack of Resilience (LoR) of a system is defined as the amount of the unmet demand of the system for a R/S over time.

4. Results and discussion

A scenario in which the community is exposed to a moment magnitude 7.4 earthquake is used to illustrate how the proposed model quantifies the seismic resilience of a community. A probability-based resilience assessment performed by running multiple scenario earthquakes is presented in [10]. Figure 4 presents the spatial distribution of the PGA due to the considered earthquake, obtained from the hazard module. The red line is the activated fault length belonging to the considered region. The maximum PGA that is observed for this scenario in the case study area is 1.397g, occurring close to locality 203.

© The 17th World Conference on Earthquake Engineering

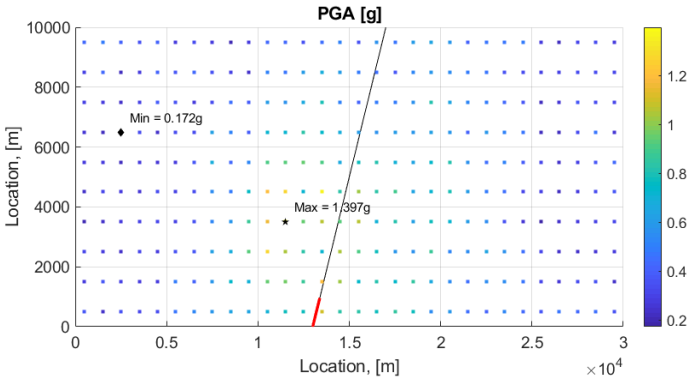

Figure 4: Spatial distribution of the PGA for the considered scenario earthquake - hazard module output

Figure 5 presents the output of the vulnerability module: the initial damage states of the CIS facilities, building stock units, pipes and bridges due to the considered scenario earthquake. Only two facilities are in damage state 4 (complete damage): the EPP and CWF at locality 305. The bridge connecting localities 201 to 301 suffered minor damage, while the bridge connecting localities 301 to 302 is not damaged.

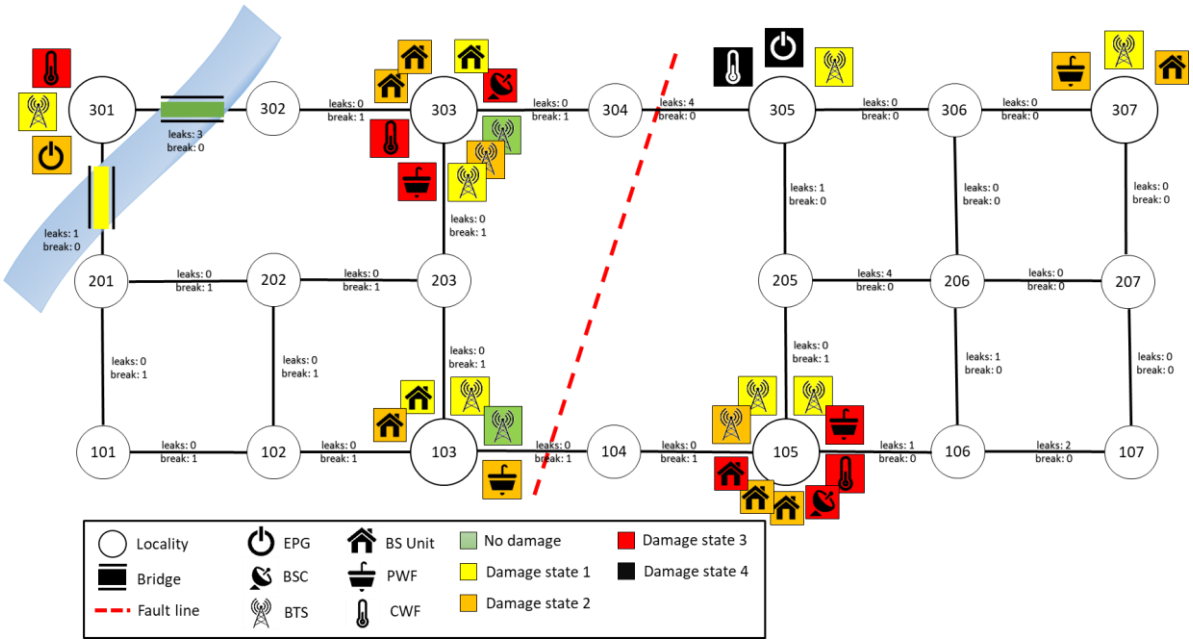

Figure 5: Initial damage state of the virtual community due to the scenario earthquake (t=0)

Figure 6 - Figure 8 present the community resilience plots for each of the considered R/Ss, where the supply capacity (i.e., how much of the considered R/S is produced in the community), demand (i.e. the demand of all the users of the considered R/S in the community) and consumption (i.e. how much of the considered R/S reached the users and is consumed by them) are plotted over the recovery period using a one day time step. The area between the consumption and the demand curve is the Lack of Resilience (LoR) – the unmet R/S demand. Two modelling cases are considered: the independent case (dashed lines), and the interdependent case (solid lines). The independent case considers only the physical damage of the components and assumes that all R/Ss provided by other CISs are available. The interdependent case considers the interdependency effects between the CISs and their components.

© The 17th World Conference on Earthquake Engineering

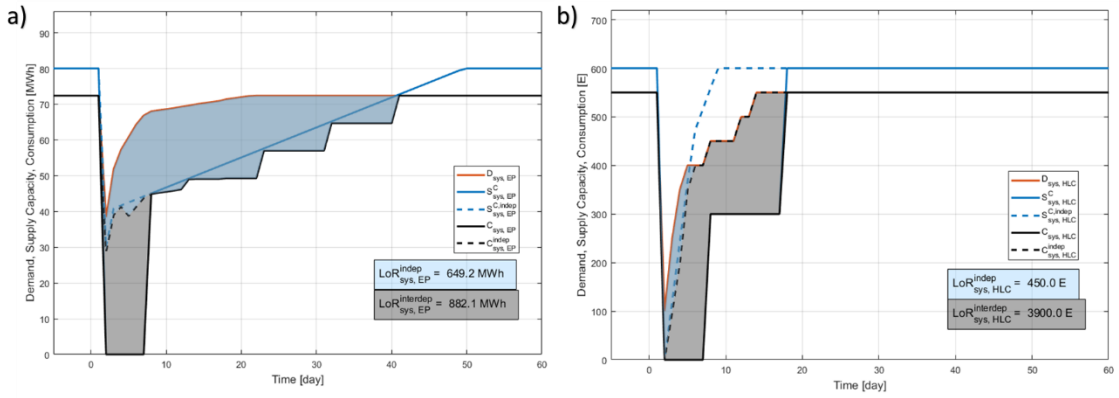

Figure 6: System resilience plot with respect to electric power EP (a) and high-level communication HLC (b) – resilience quantification module output

Figure 6a presents the supply, consumption and demand trends related to the electric power (EP) over the considered time period. The drop in the demand (red line) is due to the damage that the users of the electric power suffered (i.e. the building stock and the facilities of other CISs that require electric power to operate). As these users are recovering, the demand is increasing over time. In the independent case, the supply capacity drops from 80MWh to 30MWh immediately after the earthquake. If interdependencies are considered, the supply capacity drops to 0MWh, since EPPs demand for cooling water and cellular communication cannot be met. In this case, the EPPs demand is fully met only on day 8 after the event, after the necessary repairs of the components and links are made. The difference in the consumption (black line) – the amount of the electric power actually consumed by the users, and supply capacities (blue line) – the amount of electric power produced by the EPPs, can occur for two reasons: either the power lines are damaged and cannot transfer the electric power from the suppliers to the users, or the current demand of certain components for electric power cannot be fully met. Here, it is assumed that the demand of a component for any R/S must be met in full before the component starts to consume that R/S. For example, if in a certain time step a component demands 0.1MWh of EP, but only 0.05MWh are available to it, the demand of the component will not be met, the component will not operate at that time step, and the available 0.05MWh will be transferred to the next component according to the priority list [9]. Only when the entire 0.1MWh are available to the component, its demand will be met and the component will be operational. Since, it is assumed that the power lines cannot be damaged, the steps in the evolution of the consumption at days 13, 22, 31 and 40 are due to a sufficient increase of the supply capacity to fully meet the demand of certain components for electric power, increasing as well the consumption in the considered community.

Figure 6b shows the supply, consumption and demand evolution of the high-level communication – HLC (i.e., communication between the BTSs and the BSCs). A drop in the demand for HLC can be observed after the earthquake due to the damage suffered by the BTSs, the users of HLC. As BTSs are recovering, the demand for HLC is increasing. The difference in the supply capacity for the two modelling cases are even more evident in the case of HLC. After the earthquake, the supply capacity drops to 0E in both independent and interdependent case. The reason is that both BSCs considered in the case study are in damage state 3, for which the assumed damaged level is 100% (Table 1). The supply capacity in the independent case reaches the pre-disaster level on day 9, while the initial supply capacity is reached on day 19 in the interdependent case.

© The 17th World Conference on Earthquake Engineering

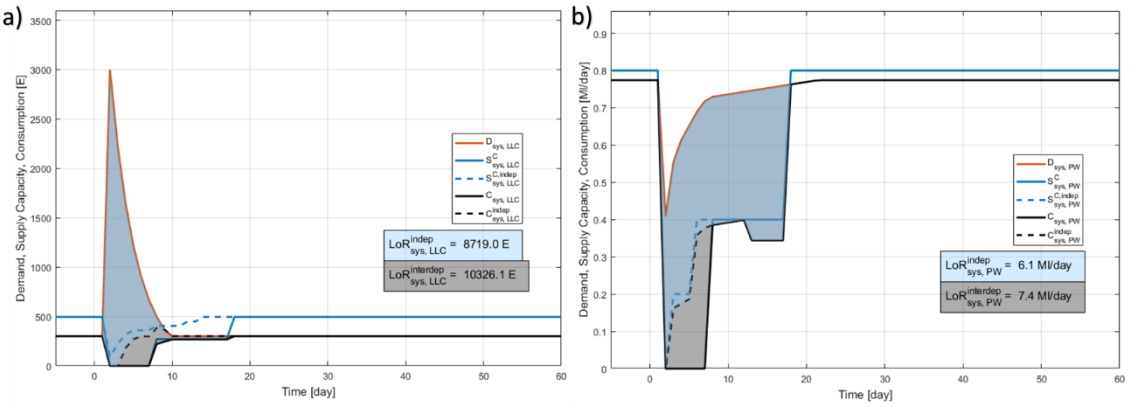

Figure 7: System resilience plot of the community with respect to the low-level communication LLC (a) and potable water PW (b) – resilience quantification module output

Figure 7a presents the supply, consumption and demand evolution for low level communication – LLC (i.e. communication between the BTSs and end users, such as building stock units). The increase in the demand for LLC is caused by the increase in the number of emergency calls following an earthquake [29, 30]. The LLC supply capacity in the interdependent case drops to zero and reaches the initial supply capacity later than it does in the independent case.

Figure 7b presents the supply, consumption and demand evolutions for potable water – PW. The drop in the demand is once again due to the damage of the users, in this case, the building stock. The interesting phenomena occurs on day 12, when the consumption drops, even though the community is recovering. This is due to the fact that a component is assumed operational only if its demand is fully met, while it is not considered as functional otherwise. In fact, between days 8 to 18, the demand increased, while the supply capacity remained constant. However, on day 12, the demand of a certain component surpassed the supply available to that component, and therefore the demand could not be fully met, lowering the consumption for potable water in the community until day 18.

Figure 8 presents the supply, demand and consumption trends regarding the cooling water – CW. The users of CW (EPPs and BSCs) are non-binary components. In this case study, such non-binary components maintain their demand for CW at no-damage level regardless of their actual damage. The jumps in the consumption, on days 4, 8 and 18 in the independent case and on days 8 and 18 in the interdependent case, are due to the pipes being repaired and due to the sufficient increase of the supply capacity so that the demand of the EPPs and BSCs can be fully met. In the interdependent case, the supply capacity is zero until day 8, since before day 8 the CWFs demands could not be met.

5. Conclusion

A compositional model for quantifying the seismic resilience of interdependent CISs was presented. The model consists of four modules: hazard, vulnerability, functional recovery and resilience quantification modules. The aim of separating the model into modules is to make the model flexible and easily upgradable. For example, if a user wants to use a different resilience quantification methodology than the one implemented here, the user can only modify the resilience quantification module, and still use the previous modules.

A virtual case study is used to illustrate the application of the presented model. A virtual community supplied with three interdependent CISs (electric power supply system, cellular communication system and water supply system) producing five types of resources and services is exposed to a scenario earthquake. Vulnerability curves from HAZUS are used to calculate the reduced functionality due to the suffered damage. However, the description of the damage states, as defined in HAZUS, does not always give information regarding the decreased functionality of the damaged components. Furthermore, the interdependency between CISs is implicitly included in the description of damage states. Therefore, models that explicitly simulate the

© The 17th World Conference on Earthquake Engineering

interdependency between CISs have a risk of double-counting the reduced functionality due to interdependency effects. The component recovery times from HAZUS are used to assess the recovery of the community.

The results from two cases are presented, one where the interdependencies are accounted for – the interdependent case, and another where the reduction of component functionality due to interdependency effects is neglected – the independent case. The lack of resilience (LoR) for each resource and service considered in the case study increased in the interdependent case, proving that interdependency, as defined in this case study, has a negative effect on the community. The difference in the LoR was from 21%, in the case of potable water, to 766%, in the case of high-level communication.

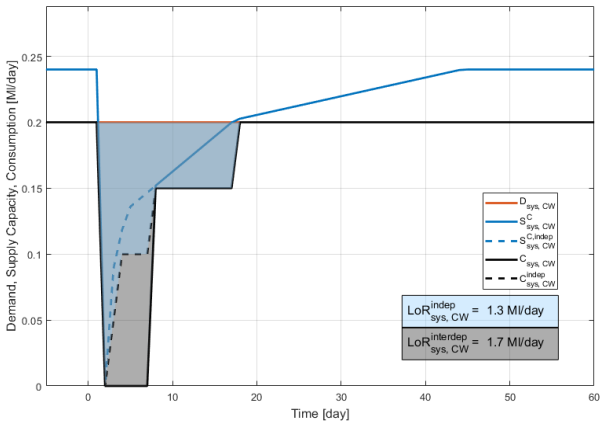

Figure 8: System resilience plot with respect to cooling water CW – resilience quantification module output

6. References

[1] OECD (2019): Good Governance for Critical Infrastructure Resilience. OECD.

[2] NIST (2014): Earthquake Resilient Lifelines: NEHRP Research, Development, and Implementation Roadmap. Technical Report *NIST GCR 14-917-33*. Applied Technology Council.

[3] US Presidential Policy Directive 21 (2013): Critical Infrastructure Security and Resilience. The White House Office of the Press Secretary.

[4] Brunner, E. and Giroux, J. (2009): CRN Report - Examining Resilience: A concept to improve societal security and technical safety. Federal Office for Civil Protection (FOCP).

[5] Risk and Resilience Measurement Committee (2019): Resilience-Based Performance: Next Generation Guidelines for Buildings and Lifeline Standards. American Society of Civil Engineers.

[6] Miles, S.B., Burton, H.V., Asce, M. and Kang, H. (2019): Community of Practice for Modeling Disaster Recovery. *Nat. Hazards Rev.* **20** (1).

[7] Bruneau, M., Chang, S.E., Eguchi, R.T., Lee, G.C., O'Rourke, T.D., Reinhorn, A.M., Shinozuka, M., Tierney, K., Wallace, W.A. and von Winterfeldt, D. (2003): A Framework to Quantitatively Assess and Enhance the Seismic Resilience of Communities. *Earthquake Spectra*. **19** (4) 733–752.

[8] Kröger, W. (2008): Critical infrastructures at risk: A need for a new conceptual approach and extended analytical tools. *Reliability Engineering & System Safety*. **93** (12) 1781–1787.

[9] Blagojevic, N., Hefti, F., Henken, J., Didier, M. and Stojadinovic, B. (2020): Quantifying Disaster Resilience of a Community with Interdependent Civil Infrastructure Systems. *Structure and Infrastructure Engineering (Submitted)*.

[10] Blagojevic, N., Kipfer, J., Didier, M. and Stojadinovic, B. (2020): Probabilistic Resilience Assessment of Communities with Interdependent Civil Infrastructure Systems. *Proc. 17th World Conference on Earthquake Engineering, 17WCEE* (Sendai, Japan).

[11] Hefti, F. (2019): *Disaster Resilience of Interdependent Civil Infrastructure Systems*. ETH Zurich.

© The 17th World Conference on Earthquake Engineering

[12] Erlang, A.K. (1925): Probability Theory Applied to Telephony. *Annales des Postes, Telegraphes et Telephones*. **4** 617–644.
[13] Bellagamba, X. (2015): *Seismic Resilience of a Gas Distribution Network*. ETH.
[14] EC8 (2003): Eurocode 8: Design Provisions for Earthquake Resistance of Structures. CEN, European Comittee for Standardisation.
[15] FEMA (2004): Hazus MH 2.1 - Technical Manual (Earthquake Model).
[16] Kramer, S.L. (1996): Geotechnical Earthquake Engineering. Prentice-Hall International Series in Civil Engineering and Engineering Mechanics.
[17] Joyner, W.B. and Boore, D.M. (1981): Peak Horizontal Acceleration and Velocity from Strong-Motion Records Including Records from the 1979 Imperial Valley, California, Earthquake. *Bulletin of the Seismological Society of America*. **74** (6) 2011–2038.
[18] Rathje, E.M. and Saygili, G. (2009): Probabilistic assessment of earthquake-induced sliding displacements of natural slopes. *Bulletin of the New Zealand Society for Earthquake Engineering*. **42** (1) 18–27.
[19] Wells, D.L. and Coppersmith, K.J. (1994): New Empirical Relationships among Magnitude, Rupture Length, Rupture Width, Rupture Area, and Surface Displacement. *Bulletin of the Seismological Society of America*. **84** (4) 974–002.
[20] Akkar, S., Sandıkkaya, M.A. and Bommer, J.J. (2014): Empirical ground-motion models for point- and extended-source crustal earthquake scenarios in Europe and the Middle East. *Bulletin of Earthquake Engineering*. **12** (1) 359–387.
[21] Esposito, S. and Iervolino, I. (2011): PGA and PGV Spatial Correlation Models Based on European Multievent Datasets. *Bulletin of the Seismological Society of America*. **101** (5) 2532–2541.
[22] Esposito, S. and Iervolino, I. (2012): Spatial Correlation of Spectral Acceleration in European Data. *Bulletin of the Seismological Society of America*. **102** (6) 2781–2788.
[23] Iervolino, I., Giorgio, M., Galasso, C. and Manfredi, G. (2010): Conditional Hazard Maps for Secondary Intensity Measures. *Bulletin of the Seismological Society of America*. **100** (6) 3312–3319.
[24] Pitilakis, K., Crowley, H. and Kaynia, A. (2014): SYNER-G: Typology Definition and Fragility Functions for Physical Elements at Seismic Risk - Buildings, Lifelines, Transportation Networks and Critical Facilities. Springer Netherlands.
[25] Steven M. Rinaldi, James P. Peerenboom and Terrence K. Kelly (2001): Identifying, understanding, and analyzing critical infrastructure interdependencies. *IEEE Control Systems*. **21** (6) 11–25.
[26] Didier, M., Broccardo, M., Esposito, S. and Stojadinovic, B. (2018): A compositional demand/supply framework to quantify the resilience of civil infrastructure systems (Re-CoDeS). *Sustainable and Resilient Infrastructure*. **3** (2) 86–102.
[27] Didier, M., Broccardo, M., Esposito, S. and Stojadinovic, B. (2018): Seismic Resilience of Interdependent Civil Infrastructure Systems. *Proc. 11th U.S. National Conference on Earthquake Engineering* (Los Angeles, USA).
[28] Didier, M., Sun, L., Ghosh, S. and Stojadinovic, B. (2015): Post-Earthquake Recovery of a Community and its Electrical Power Supply System. *Proceedings of the 5th International Conference on Computational Methods in Structural Dynamics and Earthquake Engineering (COMPDYN 2015)* (Crete Island, Greece), 1451–1461.
[29] Didier, M., Baumberger, S., Tobler, R., Esposito, S., Ghosh, S. and Stojadinovic, B. (2018): Seismic Resilience of Water Distribution and Cellular Communication Systems after the 2015 Gorkha Earthquake. *Journal of Structural Engineering*. **144** (6) 04018043.
[30] Leelardcharoen, K. (2011): *Interdependent response of telecommunication and electric power systems to seismic hazard*. Georgia Institute of Technology.

© The 17th World Conference on Earthquake Engineering